

## Synthesis of newly functionalized 1,4-naphthoquinone derivatives and their effects on wound healing in alloxan-induced diabetic mice



Silvia Helena Cardoso<sup>a,\*</sup>, Cleidijane Rodrigues de Oliveira<sup>a</sup>, Ari Souza Guimarães<sup>a</sup>, Jadiely Nascimento<sup>a</sup>, Juliano Anderson de Oliveira dos Santos Carmo<sup>b</sup>, Janylle Nunes de Souza Ferro<sup>b</sup>, Ana Carolina de Carvalho Correia<sup>b</sup>, Emiliano Barreto<sup>b,\*\*</sup>

<sup>a</sup> Laboratory of Organic Synthesis and Medicinal Chemistry (LaSOM), Núcleo de Ciências Exatas (NCEX), Campus Arapiraca, Federal University of Alagoas, CEP 57.309-005, Arapiraca, Alagoas, Brazil

<sup>b</sup> Laboratory of Cell Biology, Campus A.C. Simões, Federal University of Alagoas, CEP 57.072-970, Maceio, Alagoas, Brazil

### ARTICLE INFO

#### Keywords:

Naphthoquinone derivatives  
Wound healing  
Diabetes

### ABSTRACT

Naphthoquinone derivatives have various pharmacological properties. Here, we describe the synthesis of new 1,4-naphthoquinone derivatives inspired by lawsone and  $\beta$ -lapachone and their effects on both migration of fibroblasts *in vitro* and dermal wound healing in diabetic mice. NMR and FTIR spectroscopy aided characterization of chemical composition and demonstrated the molecular variations after the synthesis of four different derivatives, namely 2-bromo-1,4-naphthoquinone (termed derivative **S3**), 2-N-phenylamino-1,4-naphthoquinone (derivative **S5**), 2-N-isonicotinoyl-hydrazide-1,4-naphthoquinone (derivative **S6**), and 1-N-isonicotinoyl-hydrazide-[2-hydroxy-3-(3-methyl-2-butenyl)]-1,4-naphthoquinone (derivative **S7**). Our results indicate that derivatives **S3**, **S5**, **S6** and **S7** were non-toxic to the 3T3 fibroblast cell line. In scratch assays, derivatives **S3** and **S6**, but not **S5** or **S7**, stimulated the migration of fibroblasts. Compared with untreated diabetic mice, **S3**, **S6** and **S7** treatments accelerated wound closure. However, derivative **S3** was optimal for the stimulation of epithelialization, thereby increasing the number of keratinocyte layers and blood vessels, and reducing diffuse cellular infiltration, compared to derivatives **S6** and **S7**. Our results suggest that novel 1,4-naphthoquinone derivatives promote fibroblast migration and accelerate wound closure under diabetic conditions.

### 1. Introduction

Diabetes includes a heterogeneous group of disorders characterized by hyperglycemia and a relative or absolute lack of insulin secretion or action [1]. According to the World Health Organization, more than one million people die from diabetes each year, and an increasing number of patients require hospitalization. Current projections indicate that nearly 415 million adults have diabetes and that this estimate will reach 642 million individuals in 2040 [2].

Non-healing wounds are a typical hallmark of diabetes that results in chronic lesions, ulcers, and amputation of the extremities, negatively impacting patient quality of life and raising costs for health systems [3,4]. Approximately 85 million patients with diabetes worldwide have complications associated with delayed cutaneous wound healing [5].

Cutaneous wound healing is a dynamic process that requires coordinated participation of many cell types acting in distinct phases to restore the anatomical and functional integrity of tissue [6]. The wound

healing impairment seen in diabetes is a consequence of both extrinsic and intrinsic factors including repeated trauma and/or maintained hyperglycemia. Both factors negatively affect the phases of healing by interfering with cellular penetration, oxidative metabolism, collagen deposition, blood circulation, and angiogenesis [7]. Therefore, given that different cellular and molecular events are affected by diabetic conditions, a treatment based on simultaneous correction of the multiple deficits could be an attractive alternative. However, new therapeutic products with these characteristics may have side effects and/or involve high costs [8]. Thus, developing effective and economical therapies for correcting healing of diabetic wounds are still needed.

The chemical modification of existing active principles is a strategy of great importance in identifying new medicinal products [9]. Examples of successful medicines that originated from natural products include procaine, simvastatin, and dapagliflozin, among others [10]. This approach can result in new drugs capable of promoting improvements in the quality of life of diabetic patients with wounds that are slow to heal.

\* Corresponding author.

\*\* Corresponding author.

E-mail addresses: [silvia.cardoso@arapiraca.ufal.br](mailto:silvia.cardoso@arapiraca.ufal.br) (S.H. Cardoso), [emilianobarreto@icbs.ufal.br](mailto:emilianobarreto@icbs.ufal.br) (E. Barreto).

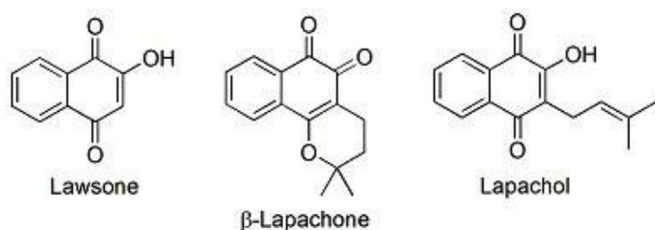


Fig. 1. Chemical structures of natural naphthoquinone derivatives.

Naphthoquinones are natural aromatic compounds that can be found in several plant families and are traditionally used for their dyeing properties [11]. However, recently, a variety of biological activities to compounds as lawsone,  $\beta$ -lapachone, and lapachol (Fig. 1), have been reported, including antimalarial, antioxidant, and antimutagenic activities [12–15].

These natural naphthoquinones have been demonstrated to have wound healing properties, which may be due to anti-inflammatory and antioxidant properties [16,17]. Additionally, a previous study demonstrated that oral administration of lawsone promoted cutaneous healing of both excision and incision wounds in rats [18]. Furthermore, previous studies have been demonstrated the influence of electron-donating or withdrawing groups into structure of 1,4-naphthoquinones able to improving their pharmacological activities [19,20]. However, to the best of our knowledge, there are no available data on the evaluation of the potential healing effects of these naphthoquinone derivatives for diabetic wounds. Thus, the present study aimed to evaluate the effects of naphthoquinones derivatives in skin wound healing in diabetic mice.

## 2. Materials and methods

Melting points were determined by the MQAPF-301 apparatus and were uncorrected. Infrared spectra were obtained using the Bomem FT-IR MB-102 spectrometer with KBr pellets.  $^1\text{H}$  NMR (400 MHz) and  $^{13}\text{C}$  NMR (100 MHz) spectra were recorded using the Bruker Advanced DPX spectrometer with  $\text{CDCl}_3$  or  $\text{DMSO}-d_6$  as the solvent. Column chromatography was performed using silica gel 60G 0.0630–200 mm (70–230 mesh ASTM) Merck and silica gel 60G 0.2–0.5 mm VETEC. TLC analyses were performed on precoated aluminum plates of silica gel 60F 254 plates (0.25 mm, Merck). Solvents were purified and dried according to the standard procedure.

Naphthoquinones were purchased from Sigma-Aldrich (USA) and were used without purification; these included 1,4-naphthoquinone (**S1**), lawsone (**S2**) (2-hydroxy-1,4-naphthoquinone), and 2-bromo-1,4-naphthoquinone (termed derivative **S3**). Lapachol (2-hydroxy-3-(3-methyl-2-butenyl)-1,4-naphthoquinone) (**S4**) was isolated from the bark of *Tabebuia* sp., collected in the Agreste Region of Alagoas State (Brazil) and used as the starting material for the synthesis of 1-N-Isonicotinoyl-hydrazone-[2-hydroxy-3-(3-methyl-2-butenyl)]-1,4-naphthoquinone (termed derivative **S7**). **S1** was used for the synthesis of 2-N-phenylamino-1,4-naphthoquinone (derivative **S5**), while **S2** was used for the synthesis of 2-N-isonicotinoyl-hydrazide-1,4-naphthoquinone (derivative **S6**).

### 2.1. Chemistry

#### 2.1.1. Extraction and characterization of lapachol (**S4**)

Lapachol was isolated from wooden chips of *Tabebuia* sp. bark by aqueous sodium carbonate extraction (10% w/v), followed by dilute hydrochloric acid precipitation and then ethanol or ethyl acetate recrystallization, leading to a 1–2% yield from the bark.  $\text{C}_{15}\text{H}_{14}\text{O}_3$ ; mp: 139–140 °C (lit. 140 °C). Yellow solid. [ $^1\text{H}$  NMR (400 MHz,  $\text{CDCl}_3$ ):  $\delta$  8.13 (1H, dd,  $J = 7.6$ ; 1.3 Hz); 8.08 (1H, dd,  $J = 7.5$ ; 1.4 Hz); 7.76 (1H, td,  $J = 7.6$ ; 1.3 Hz); 7.66 (1H, td,  $J = 7.6$ ; 1.3 Hz); 7.3 (1H, s, OH);

5.21 (1H, m), 3.32 (1H, d,  $J = 7.4$  Hz); 1.79 (3H, s); 1.69 (3H, s). NMR  $^{13}\text{C}$  (100 MHz,  $\text{CDCl}_3$ ):  $\delta$  184.6 (C=O); 181.7 (C=O); 159.9 (CH), 152.7 (C); 134.7 (CH); 133.8 (CH); 133.7 (CH); 132.7 (CH); 129.6 (C); 129.3 (C); 126.6 (CH); 119.6 (C); 25.7 (CH<sub>3</sub>); 22.5 (CH); 17.8 (CH<sub>3</sub>). FTIR: 1665 (C=O); 2917 (CH<sub>2</sub> e CH<sub>3</sub>); 1597 (C=C); 3354 (OH); 724 (CH aromatic).

#### 2.1.2. Synthesis and characterization of naphthoquinones derivatives

In order to assure novelty in the synthesis route, we perform modifications in the structure of 1,4-naphthoquinone with nitrogenated group. All target compounds were obtained by nucleophilic attack of the most basic nitrogen directly into a carbonyl group (C1) or in a carbon (C2) of 1,4-naphthoquinone.

**2.1.2.1. 2-N-phenylamino-1,4-naphthoquinone (S5).** 1,4-naphthoquinone **S1** (871 mg, 3.5 mmol) was dissolved in 60 mL of water, and after complete dissolution, it was added to 0.3 mL of aniline solution. The mixture was stirred at reflux for 24 h when the TLC consumption of the starting material was observed. Solids obtained were filtered, washed with cold water, dried, and recrystallized with methanol to obtain the derivative **S5** at 69% yield.  $\text{C}_{16}\text{H}_{11}\text{N}_1\text{O}_2$ , mp. 156–160 °C; Dark red solid, NMR  $^1\text{H}$  (400 MHz,  $\text{CDCl}_3$ ):  $\delta$  8.11 (2H, m); 7.77 (1H, td,  $J = 7.4$ ; 1.5 Hz); 7.68 (1H, td,  $J = 7.6$ ; 1.5 Hz); 7.43 (2H, t,  $J = 8.0$  Hz); 7.29 (2H, d,  $J = 8.8$  Hz); 7.23 (1H, t,  $J = 7.4$  Hz); 6.43 (1H, s), NMR  $^{13}\text{C}$  (100 MHz,  $\text{CDCl}_3$ ):  $\delta$  183.9 (C=O); 182.1 (C=O); 144.7 (C=C-N); 137.4 (C-N); 134.9 (CH); 133.2 (C); 132.3 (CH); 130.3 (C); 129.7 (CH); 126.5 (CH); 125.1 (CH); 125.6 (CH); 123.6 (CH); 122.8 (2 x CH); 103.3 (CH).

**2.1.2.2. 2-N-isonicotinoyl-hydrazide-1,4-naphthoquinone (S6).** 2-Hydroxy-1,4-naphthoquinone **S2** (2.5 g, 14.4 mmol) was dissolved in 100 mL of 80% glacial acetic acid solution. To this suspension, 1.6 g of isonicotinoyl hydrazide was added gradually. After the addition of the hydrazide, a color change was observed from yellow to red. After 72 h of constant stirring at room temperature, the solid obtained was filtered off, washed with 80% acetic acid solution and water, dried, and recrystallized from methanol to give the compound **S6** at 45% yield.  $\text{C}_{16}\text{H}_{11}\text{N}_3\text{O}_3$ ;  $P_{\text{dec}}$ . 222–224 °C; Orange solid, NMR  $^1\text{H}$  (400 MHz,  $\text{DMSO}-d_6$ ):  $\delta$  11.0 (1H, s); 9.5 (1H, s); 8.8 (2H, d,  $J = 5.9$  Hz); 8.03 (1H, d,  $J = 7.4$ ; 1.2 Hz); 7.9 (2H, dd,  $J = 7.4$ ; 1.1 Hz); 7.85–7.83 (3H, m); 7.76 (1H, td,  $J = 7.4$ ; 1.2 Hz); 5.76 (1H, s). NMR  $^{13}\text{C}$  (100 MHz,  $\text{DMSO}-d_6$ ):  $\delta$  182.7 (C=O); 181.3 (C=O); 164.3 (NHCO); 150.9 (CH); 148.7 (C=C-N); 139.6 (C); 135.4 (CH); 133.3 (CH); 132.8 (C); 130.9 (C); 126.3 (CH); 125.9 (CH); 121.8 (CH); 102.4 (C).

**2.1.2.3. 1-N-isonicotinoyl-hydrazone-[2-hydroxy-3-(3-methyl-2-butenyl)]-1,4-naphthoquinone (S7).** Lapachol **S4** (484 mg, 2.0 mmol) was dissolved in 20 mL of 10%  $\text{Et}_3\text{N}$  solution. To this solution, 5 mL of an aqueous solution of isonicotinoyl hydrazide (6.0 mmol) was added and was kept under constant stirring at room temperature. After 48 h, TLC consumption of the starting material was observed and the reaction was treated with 4 mL of glacial acetic acid. A solid was obtained by the precipitation of the medium using ice water; this was filtered and recrystallized from ethanol to obtain the derivative **S7** at 95% yield.  $\text{C}_{22}\text{H}_{20}\text{N}_3\text{O}_3$ ; mp 164–167 °C; Orange solid, NMR  $^1\text{H}$  (400 MHz,  $\text{DMSO}-d_6$ ):  $\delta$  16.4 (1H, sl, NH); 8.90 (2H, d,  $J = 5.5$  Hz); 8.10 (1H, sl); 7.98 (1H, sl); 7.86 (2H, d,  $J = 5.5$  Hz); 7.56 (2H, m); 5.08 (1H, m); 3.24 (2H, d,  $J = 7.2$  Hz) 1.73 (3H, s); 1.65 (3H, s). NMR  $^{13}\text{C}$  (100 MHz,  $\text{DMSO}-d_6$ ):  $\delta$  179.7 (C=O); 166.4 (C-OH); 15.5 (NHCO); 150.9 (CH); 140.3 (C); 131.3 (C, C=N); 130.9 (C); 130.4 (CH); 129.4 (CH); 127.9 (C); 124.3 (CH); 123.3 (CH); 122.4 (CH); 121.7 (CH); 117.4 (C); 25.4 (CH<sub>3</sub>); 21.2 (CH<sub>2</sub>); 17.9 (CH<sub>3</sub>).

## 2.2. Biology

### 2.2.1. Cell culture

The mouse fibroblast cell lines 3T3 were maintained in Dulbecco's Modified Eagle Medium (DMEM) supplemented with 10% fetal bovine serum, 2 mM-glutamine, and 40 µg/mL gentamicin, and cultured in a humidified atmosphere contained 5% CO<sub>2</sub> incubator at 37 °C. For the experiments, cells were grown for 24 h in supplemented medium in a 96-well cell culture plate. The assay was performed using cells between 3 and 5 passages. In all experiments, untreated cells were used as negative controls.

### 2.2.2. Cell viability assay and treatment

The effect of naphthoquinone derivatives on cell viability was evaluated by the MTT assay [22]. Naphthoquinone derivatives were dissolved in dimethyl sulfoxide (DMSO) and then diluted with DMEM. Cells were plated in 96-well plates (6 × 10<sup>3</sup>/well) and treated with naphthoquinone derivatives at concentrations of 1, 5, 10, or 50 µM, for 24 h. Thereafter, the medium was replaced with fresh RPMI containing 5 mg/mL MTT. Following an incubation period (3 h) in a humidified CO<sub>2</sub> incubator at 37 °C and 5% CO<sub>2</sub>, the supernatant was removed and dimethyl sulfoxide solution (DMSO, 150 mL/well) was added to each cultured plate. After incubation at room temperature for 15 min, the absorbance of the solubilized MTT formazan product was spectrophotometrically measured at 540 nm. Three individual wells were assayed for each treatment and the percentage viability relative to the control sample was determined as (absorbance of treated cells/absorbance of untreated cells) × 100%.

### 2.2.3. In vitro scratch wound healing assay

To evaluate the effect of naphthoquinone derivatives on fibroblast motility, we used the scratch assay as described by Herrera, Kantarci, Zarrough, Hasturk, Leung and Van Dyke [23]. Cells were maintained in 24 well plates until they reached 90% confluency. Thereafter, a vertical stripe on the cell monolayer was made using a sterile pipette (200 µl) tip. The wells were washed with PBS to remove dead cells and debris, and then naphthoquinone derivatives were added at a concentration of 10 µM. As a control, the cells were treated with cell culture medium. After 24 h of treatment, cells were photographed using an inverted microscope (Olympus IX70) with digital camera aid to measure the wound closure area. Cell migration was analyzed using Image J software and expressed as the area in pixels per field analyzed.

### 2.2.4. Animals

Experiments were carried out on adult male Swiss mice (25–35 g) obtained from the Federal University of Alagoas (UFAL) breeding unit. The animals were maintained with free access to food and water and kept at 22–28 °C with a controlled 12-h light/dark cycle at the Institute of Biological and Health Sciences (UFAL). Experiments were performed during the light phase of the cycle. All experiments were carried out in accordance with institutional guidelines and ethics (License Number 050/2013).

### 2.2.5. Induction of diabetes mellitus

Diabetes mellitus was induced in 12-h-fasted mice by an injection in the orbital venous plexus of alloxan monohydrate (65 mg/kg) dissolved in sterile saline (0.9%, NaCl) as described previously [24]. Control mice were injected only with saline. Blood glycaemia of the samples obtained from the tail vein was determined using a glucose monitor. Only mice with glucose levels above 200 mg/dL was considered to be diabetic, and those animals were included in the experiment.

### 2.2.6. Excision wound model and treatment

Twenty-one days after alloxan injection, period which stabilization of diabetes was ensured, animals were anesthetized using an intraperitoneal injection of a ketamine (100 mg/kg) and xylazine (10 mg/

kg) mixture. Thereafter, the dorsal region was shaved, wiped topically with distilled water, and circular wounds were made using a template of metal circle with a diameter of 1 cm. Animals were housed individually in disinfected cages after recovery from anesthesia and maintained during experiments. Animals were randomly divided into five groups of 5 animals: non-diabetic animals (NDB) treated with 50 µl of PBS, diabetic animals (DB) treated with 50 µl of PBS, diabetic animals (DB) treated with 50 µl of 2-bromo-1,4-naphthoquinone (**S3**, 50 µmol/kg), diabetic animals (DB) treated with 50 µl of 2-N-isonicotinoyl-hydrazide-1,4-naphthoquinone (**S6**, 50 µmol/kg), and diabetic animals (DB) treated with 50 µl of 1-N-isonicotinoyl-hydrazide-[2-hydroxy-3-(3-methyl-2-butenyl)]-1,4-naphthoquinone (**S7**, 50 µmol/kg). All animals received topical treatment on the wounds once daily until the end of the experiments.

### 2.2.7. Wound closure measurements

Macroscopic evaluation of the wounds was performed using a digital camera, on day 0 (before the start of treatment) and on 3rd, 6th, 9th, and 12th days after injury, and the data were analyzed using Adobe Photoshop CS5 software. The results of wound measurements on various days were expressed as percentage of wound closure. The wound closure percent was calculated using the following equation: [(A0 – AI)/A0 × 100], where A0 is the initial wound area (day 0) and AI is the wound area on 3rd, 6th, 9th, or 12th after initial wound.

### 2.2.8. Histopathological analysis

The new full-thickness skin layer that was regenerated by 12 days post wounding was removed using a surgical scalpel for histological analysis. Animals were euthanized with thiopental sodium (100 mg/kg, i. p.) to collect granulation/healing tissue. The skin specimens were fixed in 10% buffered formalin, processed, and blocked with paraffin [25]. Then, sample were sectioned into 5-µm-thick sections and stained with hematoxylin and eosin (H&E), as per the standard method and visualized under a light microscope (Olympus BX51 attached DP70 Digital Camera System) at 10× and 40× magnification.

### 2.2.9. Statistical analysis

Data were expressed as mean ± standard deviation. The statistical analysis involving two groups was done using Student's *t*-test. Analysis of variance followed by the Tukey's test were used to compare three or more groups. Values of *p* < 0.05 were considered as indicative of significance.

## 3. Results

### 3.1. Synthesis of naphthoquinones derivatives

The strategy for the synthesis of *N*-substituted-naphthoquinones **S5**, **S6**, and **S7** is presented in Fig. 2. All compounds were obtained in yields ranging from satisfactory to excellent by nucleophilic attack of the most basic nitrogen directly into the carbonyl group (C1) or into a carbon (C2) of the 1,4-naphthoquinone nucleus and were characterized by adequate spectroscopic techniques, Fig. 2.

### 3.2. FTIR spectra

In this study, FTIR data were used to identify the major functional groups present in the compounds. In general, FTIR spectra of products showed the stretching vibrations of OH, NH, and NH<sub>2</sub> groups binding were observed in the 3440–3200 cm<sup>-1</sup> region. In the starting material 1,4-naphthoquinone, lawson or lapachol the bands of two carbonyl groups  $\nu(^1\text{C}=\text{O})$  and  $\nu(^4\text{C}=\text{O})$  and stretching vibrations of C–O were observed in the 1660–1640 cm<sup>-1</sup> and 1224–1047 cm<sup>-1</sup> regions, respectively. In the **S3** derivative, the stretching vibrations of C–Br was observed at 690 cm<sup>-1</sup>. For the 2-*N*-substituted-naphthoquinones **S5** and **S6**, the bands of the carbonyl groups  $\nu(^1\text{C}=\text{O})$  and  $\nu(^4\text{C}=\text{O})$  were

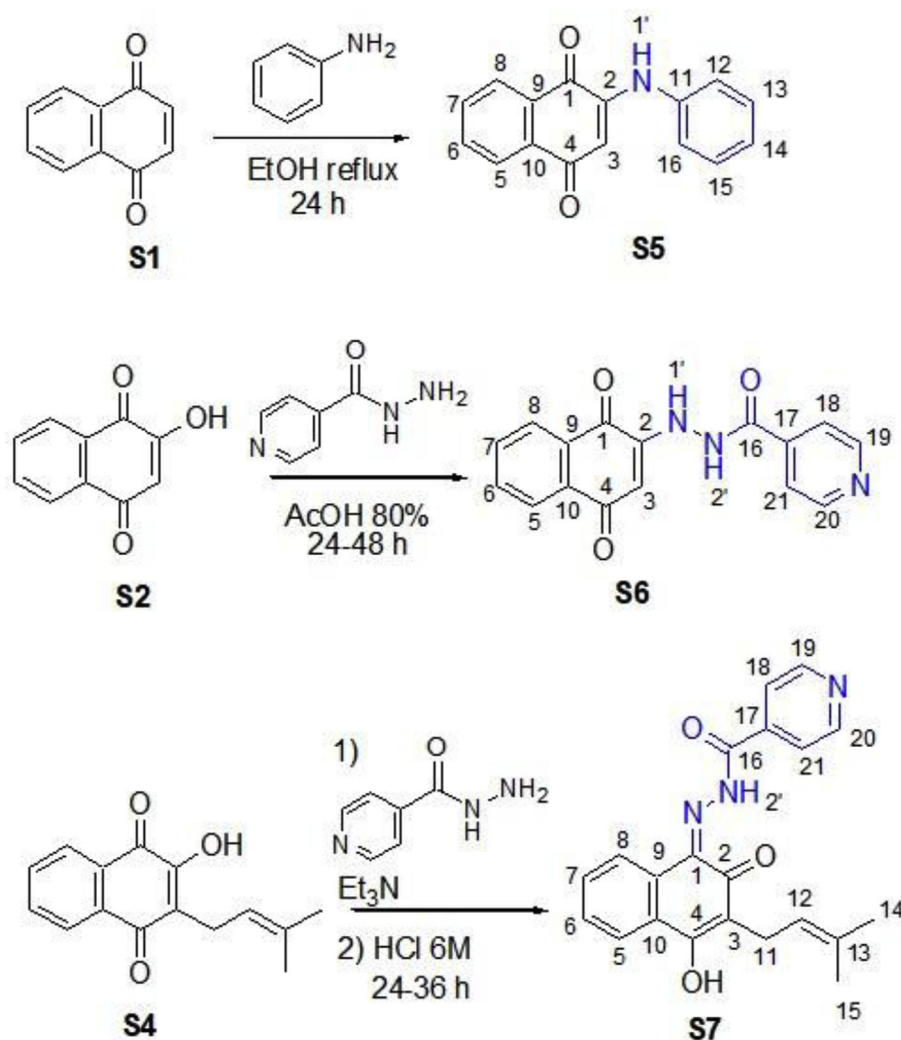


Fig. 2. Strategy of synthesis of N-substituted-1,4-naphthoquinones **S5**, **S6** and **S7**.

observed in the 1673–1660  $\text{cm}^{-1}$  region, while the stretching vibrations of C–N appeared in the 1670–1343  $\text{cm}^{-1}$  region. For **S7**, a 1-N-acylhydrazone, was observed the appearance of an absorption band which can be attributed to the formation of the C=N bond was observed. The  $\nu(\text{C}=\text{N})$  was observed in the 1681–1545  $\text{cm}^{-1}$  region.

### 3.3. $^1\text{H}$ NRM spectra

$^1\text{H}$  NMR spectroscopic analysis of the compounds **S3–S7** showed signals concerning the aromatic hydrogens of the naphthalene ring system between  $\delta$  8.1–7.8 ppm as doublets and triplets. The singlet corresponding to the hydrogen CH (H3), proton neighboring the bromo group appears at  $\delta$  7.5 ppm. In **S5**, this hydrogen, neighboring the aniline group, was observed at  $\delta$  6.4 ppm and in **S6** the proton (H3) appears at 5.7 ppm. The chemical shift of this proton can be explained in terms of the presence of electron donor or electron withdrawal groups connected to the conjugate system. For **S7**, this signal is absent due to the presence of the isoprenyl side-chain at C3. Regarding the isonicotinoyl hydrazide group present in **S6** and **S7**, the four pyridyl protons could be assigned at 8.8 and 7.8 ppm, the two ortho protons with respect to nitrogen (H19 and H21, Fig. 2) are largely deshielded. In **S6**, the two singlets observed at approximately 9.6 and 11.0 ppm are due to the N (1')H and N (2')H groups (Fig. 2). In addition, the presence of the N (1')H chemical shift at 11.0 ppm in **S6** was indicative of conformation in which N (1')H is hydrogen bonded to the carbonyl oxygen

( $^1\text{C}=\text{O}$ ).

The comparison of  $^1\text{H}$  NMR spectra between the starting material and the **S7** derivative indicated that the signals from the side-chain at C3 were virtually unchanged. The presence of a largely deshielded signal at 16.4 ppm in the **S7** spectra was indicative of conformation in which N (2')H is hydrogen bonded to the carbonyl oxygen ( $^2\text{C}=\text{O}$ ). It is expected that **S7** will adopt the *E* or *Z* conformation in solution. In this type of reaction, *E*- and *Z*-acylhydrazones are in equilibrium through the intermediate hemiaminal (Fig. 3). In this study,  $^1\text{H}$  NMR data indicated that only one of two possible diastereoisomers was formed with the *Z*-stereochemistry for the C=N double bond in **S7**. *Z*-stereochemistry was established by the intramolecular N (2')–H...O=C six-membered hydrogen-bonded ring.

### 3.4. $^{13}\text{C}$ NMR spectra

$^{13}\text{C}$  NMR spectra of **S5** and **S6** showed the two carbonyl groups ( $\text{C}=\text{O}$ ) between  $\delta$  183.7–181.8 ppm, which demonstrates that the 1,4-naphthoquinone nucleus was preserved and the substitution of the nitrogenous group occurred at the C2 carbon. In addition, in **S5** and **S6** the  $\text{C}=\text{C}-\text{NH}$  was observed at  $\delta$  144.7 and 148.7 ppm, respectively. The aromatic carbons of **S5** were observed between  $\delta$  134.8–122.1 ppm. In the  $^{13}\text{C}$  NMR spectra of **S7**, an 1-N-acylhydrazone, the signals at  $\delta$  179.6 and 166.4 ppm were attributed to the carbonyl ( $^2\text{C}=\text{O}$ ) and  $^4\text{C}-\text{OH}$  groups, respectively. These signals result from the structural

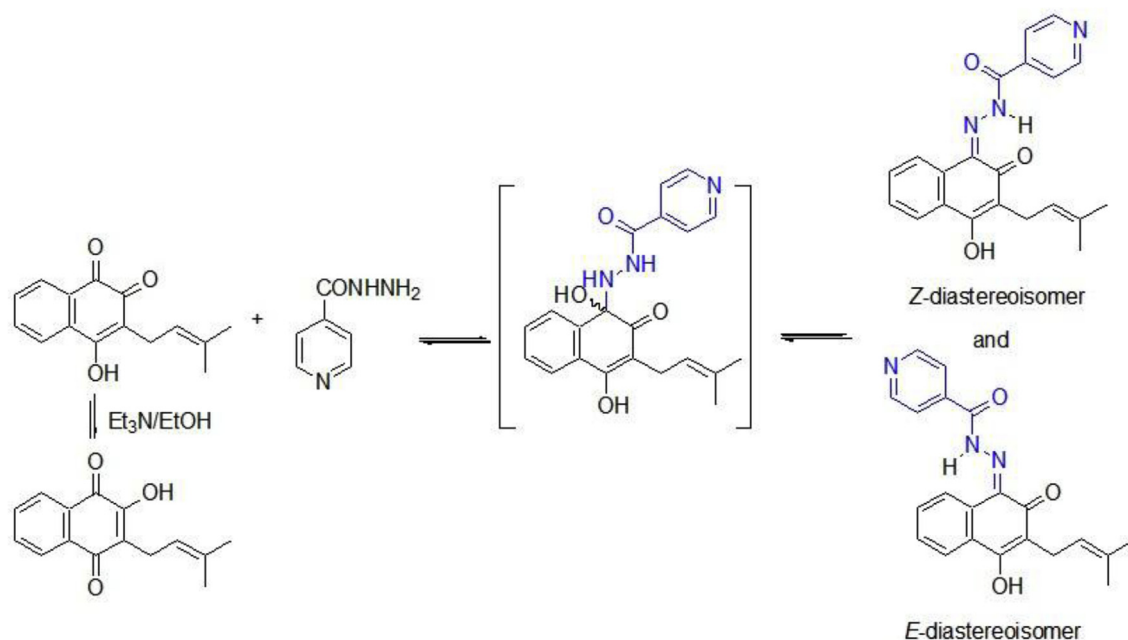


Fig. 3. Equilibrium of *E* and *Z*-hydrazones through intermediate hemiaminals.

modification of the naphthoquinone nucleus that occurred after the insertion of the isonicotinoyl hydrazide group. The signal of the carbon in the hydrazone group ( $^1\text{C} = \text{NNCOR}$ ) was observed at  $\delta$  131.0 ppm. The four carbons of the pyridyl groups in **S6** and **S7** were observed at  $\delta$  150.8 and 121.9 ppm, as well as a carbonyl group of amide at  $\delta$  164.1 and 159.9 ppm, respectively. The COSY and HMBC spectra were used to confirm the structures and unambiguously assign the chemical shifts for all the hydrogen and carbon atoms.

### 3.5. Effects of naphthoquinone derivatives on cell viability

Because naphthoquinone derivatives could have toxic activities, we first evaluated the cytotoxicity of these compounds using an MTT assay. As shown in Fig. 4, there was a significant reduction in the viability of 3T3 cells after treatment with 1,4-naphthoquinone **S1** and lapachol **S4**,

but not with lawsone **S2**. Moreover, it should be noted that the naphthoquinone derivatives **S3**, **S5**, **S6**, and **S7** did not present a significant decrease in cell viability at the tested doses. On the basis of these results, we selected the compounds **S3**, **S5**, **S6**, and **S7** to proceed to the next step and evaluate their respective effects on cell migration.

### 3.6. Effects of naphthoquinone derivative exposure on fibroblast motility

The effect of naphthoquinone derivatives on migratory activity was performed with 3T3 mouse fibroblast cells using a scratch assay. Scratches were made on confluent cells and then treated with RPMI-medium (control) or naphthoquinone derivatives at a concentration of 10  $\mu\text{M}$  for 24 h. As shown in Fig. 5, the treatment of fibroblasts for 24 h with the naphthoquinone derivatives **S3** and **S6** accelerated the wound closure area by approximately 56% and 68%, respectively. However,

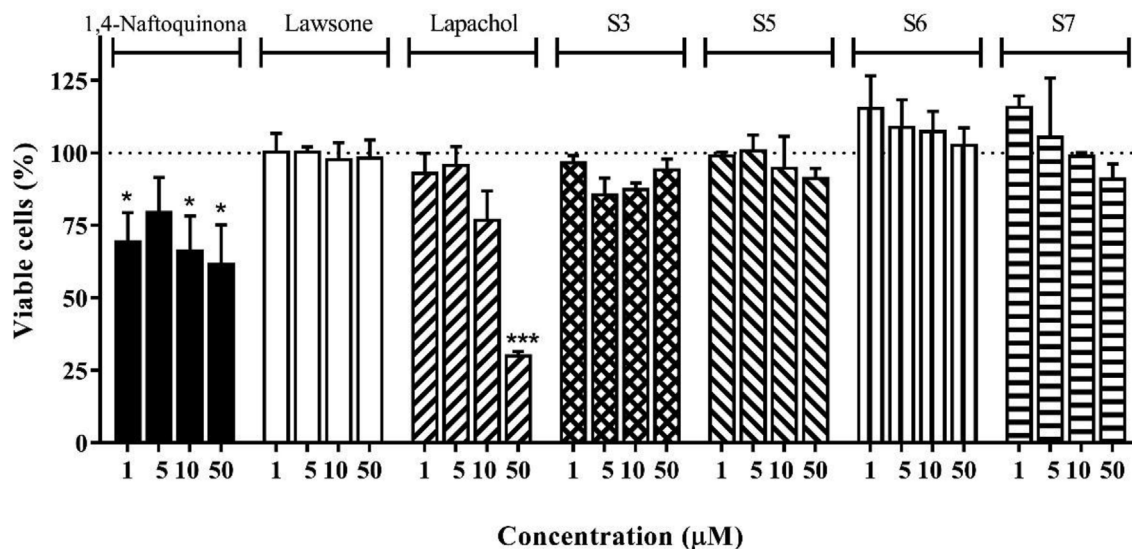
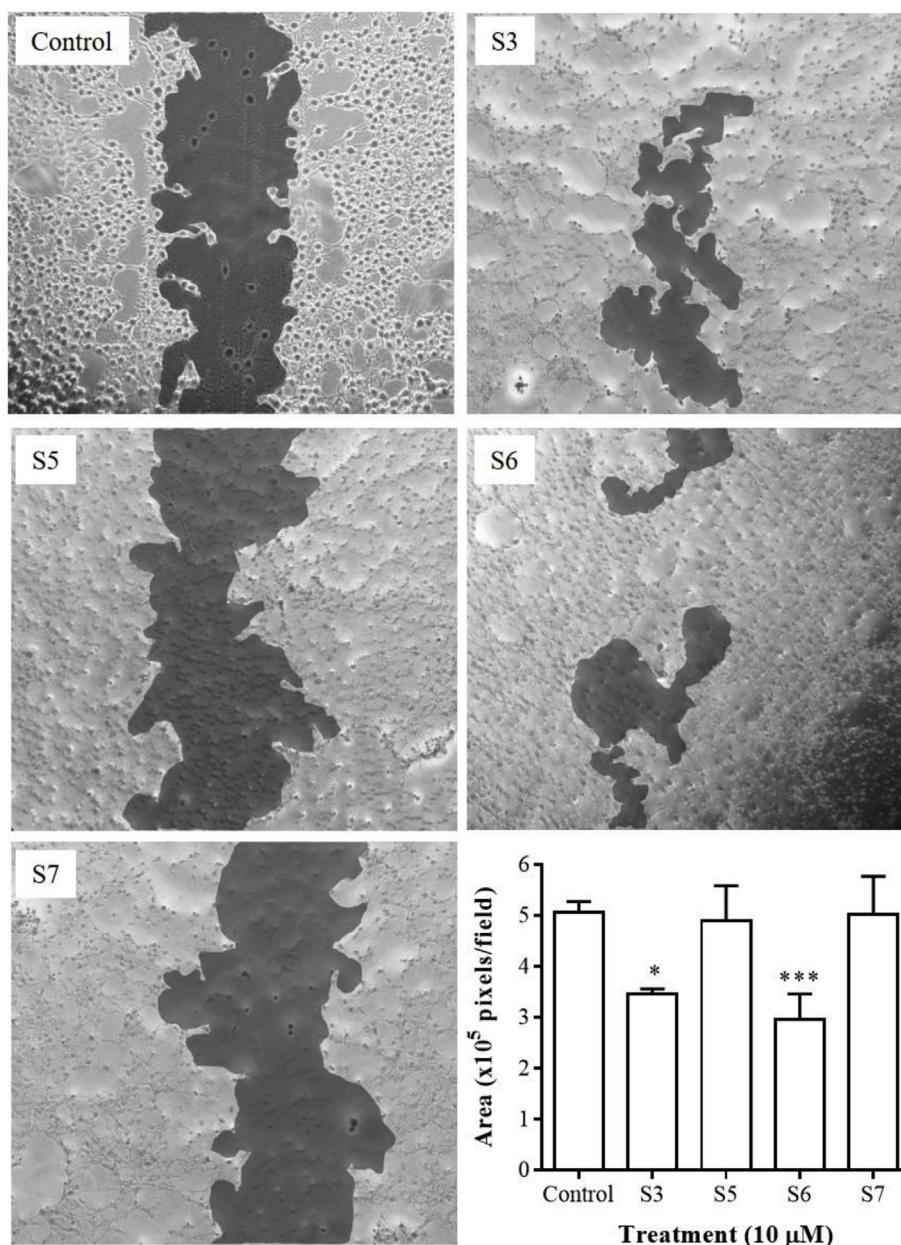


Fig. 4. The viability of 3T3 cells after 24 h naphthoquinone derivatives exposure. The dotted line represents the control group (cells treated with DMEM) and bars represent the mean  $\pm$  S.D. One-way ANOVA was used with Tukey test, where a p-value  $< 0.05$  was deemed statistically significant. \*p  $< 0.05$  and \*\*\*p  $< 0.001$  vs control group.



**Fig. 5.** Effect of naphthoquinone derivatives in closure of scratched areas in the scratch assay. Representative photomicrographs of the wounded cells at 24 h after the scratch, and quantitative analysis of area closed in scratch assay expressed as percentage of initial area. Bars represent mean  $\pm$  S.D. One-way ANOVA was used with Tukey test, where a p-value  $< 0.05$  was deemed statistically significant. \* $p < 0.05$  and \*\* $p < 0.01$  vs control group.

cells treated with naphthoquinone derivatives **S5** and **S7** exhibited a profile of wound closure area similar to the untreated cells (control), indicating no effect of this derivative on the migratory capacity of fibroblasts. On the basis of these results, we evaluated the effects of these derivatives on an *in vivo* wound-healing model. It is important to emphasize that, although the derivative **S7** did not show an effect on fibroblasts in the scratch assay, we decided include this derivative in the *in vivo* test due to its structural similarity to derivative **S6** (isonicotinoyl group) and the fact that **S7** has not previously been described in the literature.

### 3.7. Effects of naphthoquinone derivatives on *in vivo* wound healing assay

Here, the excision wound model was used in order to assess healing activity of the naphthoquinone derivatives **S3**, **S6**, and **S7** in mice with diabetes induced with alloxan. The progression of healing was

evaluated on days 3, 6, 9, and 12 post wounding.

As shown in Fig. 6A and B, the diabetic mice (DB) presented a significant delay in wound closure kinetics compared to the non-diabetic mice (NDB) at all times analyzed. When the alloxan-induced diabetic mice were topically treated with the naphthoquinone derivatives **S3**, **S6** or **S7**, an improvement in wound closure compared to the PBS-treated diabetic animals was observed on 6th, 9th, and 12th days post wounding (Fig. 6A and B). Notably, treatment with **S3**, **S6** or **S7** presented a similar effect on diabetic wound closure on day 6 with 36.7%, 35.1%, and 32.7% wound closure, respectively (Fig. 6B). However, on day 9 improved healing effects were produced by naphthoquinone derivatives **S3** and **S6**, with 82.7% and 78.1% wound closure, respectively. The **S7**-treated wound had a wound closure rate of only 61% on the 9th day.

We further examined the effects of naphthoquinone derivatives on tissue regeneration in wounds. Randomly selected photographs of

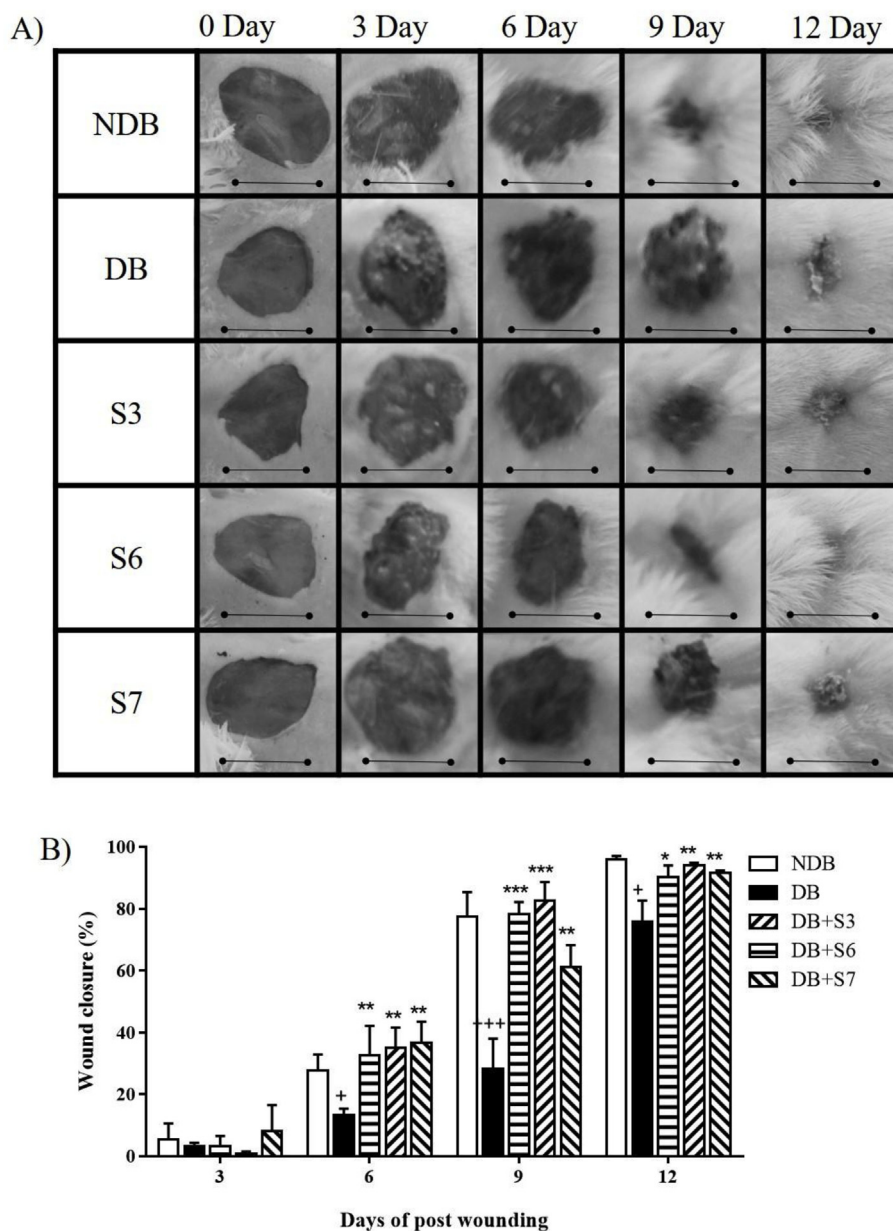


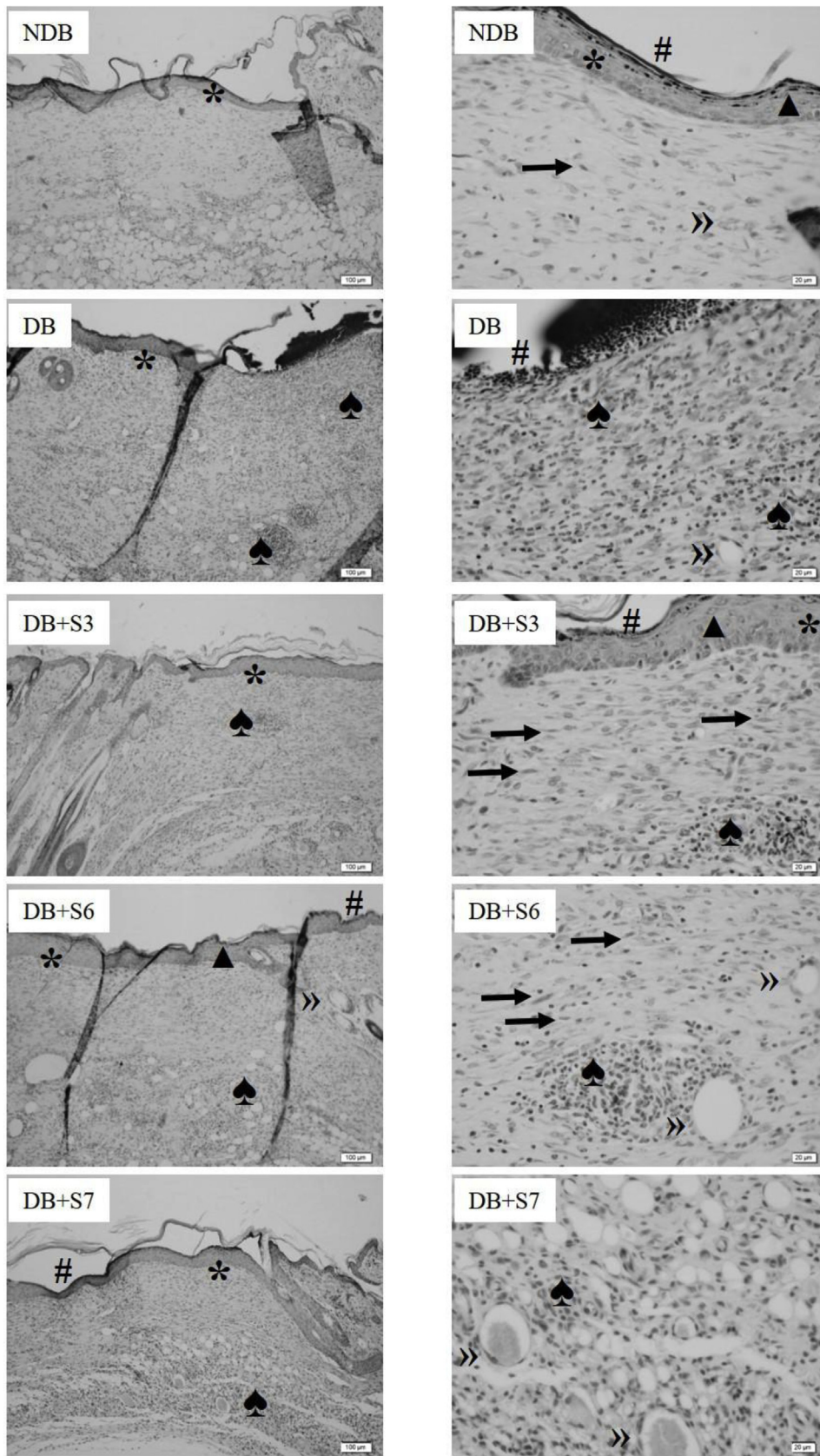
**Fig. 6.** Effect of topical application of naphthoquinone derivatives in the excisional wounds in diabetic mice. (A) Representative photographs of wounds at days post wounding of non-diabetic animals (NDB), diabetic animals (DB), diabetic animals treated with **S6** (DB+S6), and diabetic animals treated with **S3** (DB+S3). (B) Wound closure kinetics. Bars represent mean  $\pm$  S.D. One-way ANOVA was used with Tukey test. +p < 0,05, ++p < 0,01, and +++p < 0,001 compared to NDB group. \*\*p < 0.01 and \*\*\*p < 0.001 compared to DB group.

wound tissue on day 12 of non-diabetic (NDB) and diabetic (DB) mice treated with PBS, and diabetic mice treated with **S3** (DB+S3), **S6** (DB+S6), or **S7** (DB+S7) are shown in Fig. 7. Skin sections from non-diabetic animals (NDB) showed an intense epithelialization at 12 days post wounding, accompanied by a layer of keratinocytes and mature granulation tissue with blood vessels and cells showing a fibroblast-like morphology (Fig. 7, NDB). In diabetic mice (DB), the epithelialization was not complete, with an intense accumulation of inflammatory cells and a thin fragile layer of epithelium and keratinocytes (Fig. 7, DB). The histological profile of skin from diabetic animals treated with the compounds **S3** or **S6** brought an increase in the number of layers of epithelialization, accompanied by a reduction in the accumulation of inflammatory cells and the presence of fibroblast-like cells (Fig. 7, DB+S3 and DB+S6). In wounds on diabetic mice treated with **S7**, despite the improvement in wound closure revealed by a thin layer of epithelialization, absence of fibroblast-like cells and diffuse accumulation of

inflammatory cells were still observed (Fig. 7, DB+S7).

#### 4. Discussion

Delayed skin wound healing in diabetes remains as an important clinical problem, leading to prolonged hospitalization and even amputation. Consequently, obtaining chemical entities by synthesis or semi-synthesis remains as effective way to obtain new drugs with healing effects. In this study, new derivatives from 1,4-naphthoquinones were synthesized and characterized and their biological effects evaluated on an *in vitro* model of cell migration (scratch assay) and on wound healing in alloxan-induced diabetic mice. Our results provide the first evidence that two of the naphthoquinone derivatives evaluated in this study (**S3** and **S6**) act directly on fibroblasts by increasing their migratory activity *in vitro*. Moreover, we also demonstrated that naphthoquinone derivatives **S3**, **S6**, and **S7** effectively promote diabetic wound closure.



10× Magnification

40× Magnification

**Fig. 7.** Representative images of histopathological sections stained with H&E from non-diabetic (NDB) mice, diabetic mice topically treated with PBS (DB) or 50 μmol/kg naphthoquinone derivatives S3, S6 or S7 during 12 days. Set of images in on the left panel represents 10× magnification with scale bar 100 μm, while the set of images on the right panel represents 40× magnification and scale bar 20 μm. (▲) total reepithelization; (\*) multi-stratified epithelium; (#) layer of keratinocytes; (→) fusiform cells (fibroblast-like cells); (») blood vessels; (♣) diffuse cellular infiltration.

Indeed, 1,4-naphthoquinones are widely distributed in nature. They are structurally related to naphthalene and characterized by their two carbonyl groups in the 1,4 positions, leading to the name 1,4-naphthoquinones. Naphthoquinones are highly reactive organic compounds and have been shown to have important pharmacological properties, such as antimalarial, antibacterial, antifungal, and anticancer properties [12,13]. However, despite this wide range of effects, studies on the effects of non-natural naphthoquinone derivatives in wound healing remain scarce. Only a small number of natural naphthoquinones, such as alkannin and shikonin, have been studied and demonstrated wound healing properties [26,27].

Here we describe a method for the synthesis of *N*-substituted-naphthoquinones. The reaction of 1,4-naphthoquinone **S1** with aniline furnished 2-*N*-phenylamino-1,4-naphthoquinone, derivative **S5**. The reaction of 2-hydroxy-1,4-naphthoquinone **S2** with *N*-acylhydrazide (isoniazide) in an acid medium led to 2-*N*-acylhydrazino-1,4-naphthoquinone, derivative **S6**. In contrast, the reaction in a weakly alkaline solution led to 1-*N*-acylhydrazono-2-hydroxy-1,4-naphthoquinone, derivative **S7**. In this case, the formation of the conjugate base in alkaline solution was proposed to explain this behavior. The findings of the present study are in agreement with those reported by Carroll et al. [28] and Campos et al. [29].

The chemical reactivity of the 1,4-naphthoquinone nucleus is an example of an  $\alpha,\beta$ -unsaturated substance. Due to this characteristic, they have ambident behavior when reacting with nucleophiles, being able to undergo  $\beta$ -olefinic attack (1,4 addition) or direct addition to the carbonyl (1,2-addition). The preferred position of the addition will depend on the nature of the nucleophile and the reaction conditions [30].

Naphthoquinones are involved in oxidative processes due to their structural properties and their capacity to generate reactive oxygen species [31]. Moreover, the mechanism of action and pharmacological properties of these substances are dependent on their acid-base and oxide-reduction properties, which can be modulated by the structural modification of the quinone nucleus by the introduction of various substituents.

Previous studies showed that naphthoquinone derivatives are potentially toxic [32], and several studies have shown that changes in the structure of molecules cause reduction in its cytotoxicity [33], improve its biological effects [34], or even reveal new activities. Notably, conjugation of naphthoquinones with gold nanoparticles can reduce the cytotoxicity of these compounds [35]. Our results in the cytotoxicity assay showed that derivatives, in particular **S3**, **S5**, **S6**, and **S7**, have low toxicity compared to 1,4-naphthoquinone. This low cytotoxicity of the compounds might be explained by a possible change in solubility of molecules; however, further studies are required to clarify this aspect.

Fibroblasts are important cells in normal wound healing; they produce extracellular matrix and collagen structures that support the other cells associated with effective wound healing [36]. In addition, the ability of fibroblasts to migrate is an extremely important feature during the granulation tissue formation phase of wound healing [37]. One way of assessing the interference of compounds on cell migration is the scratch assay. This method is a simple and direct way to measure the rate of cell migration in an *in vitro* wound model. Once the cell monolayer is disrupted, the loss of cell-cell interaction induces secretion of growth factors and cytokines at the wound edge, initiating migration and proliferation of cells [38].

In the present study, fibroblasts treated with naphthoquinone derivatives **S3** and **S6** induced an enhanced migration capacity leading to improved closure of the scratched area, suggesting that these derivatives have a direct effect on fibroblasts. These results are consistent with a previous study in which another naphthoquinone derivative, 2,3-dimethoxy-1,4-naphthoquinone, significantly improved fibroblast motility, a phenomenon that involved the lysophosphatidic acid signaling pathway [39]. In addition,  $\beta$ -lapachone, a natural *o*-naphthoquinone, exhibited an inductor effect on the migration of mouse 3T3 fibroblasts

through different MAPK signaling pathways [40]. Thus, these observations support the notion that derivatives **S3** and **S6** may directly affect fibroblast migration; however, future studies are required to determine the molecular mechanisms underlying the effects of these derivatives.

Diabetes is associated with altered skin wound healing [3,4]. This deficiency in healing may be associated with a persistence of inflammatory cells in the wound area, which causes tissue damage and impairs wound resolution [41,42]. As already demonstrated, hyperglycemia and oxidative stress induce excessive proinflammatory cytokine production, sustaining an infiltration of leukocytes in injured tissue from diabetic mice [43–45]. As shown in the present study, diabetic wounds still contained a large number of inflammatory cells infiltrated into tissue on day 12 after wounding, while non-diabetic wounds already exhibited an advanced stage of healing. Topical application of naphthoquinone derivatives **S3** and **S6** significantly attenuated the infiltration of inflammatory cells, which suggests these compounds might provide a favorable microenvironment for wound healing. The concept that attenuating the inflammatory response can accelerate diabetic cutaneous wound healing has previously been demonstrated using other topical treatments [46]. Considering this proposal, we cannot dismiss the effect of these naphthoquinone derivatives in accelerating each phase of the healing process, which would result in faster closure of wounds. In addition, previous reports have demonstrated that arnebin-1, a naphthoquinone derivative, accelerates the wound closure process in distinct models of delayed healing, due to the induction of expression of eNOS, VEGF, and HIF-1 $\alpha$  [47,48]. Thus, it is possible that these mediators also play a role in the naphthoquinone derivative-mediated wound healing process. Although the derivative **S7** did not show a direct effect on fibroblast migration *in vitro*, when topically applied to a wound in alloxan-induced diabetic mice, this derivative promoted an improvement in skin wound closure. However, microscopic analysis revealed a weak reduction in the accumulation of inflammatory cells. These differentiated effects induced by the naphthoquinone derivatives could be attributed to the actions at distinct targets at the injury site. Therefore, although speculative, this idea cannot be dismissed. Further studies are required to investigate this concept.

## 5. Conclusion

Based on the outcomes of the present study, we demonstrated that naphthoquinone derivatives **S3** and **S6**, but not **S7**, improve fibroblast migration *in vitro*. However, the topical application of **S3**, **S6**, and **S7** accelerated the wound healing process in alloxan-induced diabetic mice. Taken together, we conclude that naphthoquinone derivatives may have potential as a healing-promoting agent for wound healing, particularly under diabetic conditions.

## Acknowledgements

The authors are grateful to the research team at the Laboratory of Cell Biology and LaSOM for helping them with some experimental protocols. This study was supported by the Brazilian Ministry of Health and Fundação de Amparo à Pesquisa do Estado de Alagoas/SUS Research Program (FAPEAL/PPSUS) [grant number 60030000712/2013]. Authors thank Coordenação de Aperfeiçoamento de Pessoal de Nível Superior and Conselho Nacional de Desenvolvimento Científico e Tecnológico by the scholarships.

## Appendix A. Supplementary data

Supplementary data related to this article can be found at <http://dx.doi.org/10.1016/j.cbi.2018.06.007>.

## Transparency document

Transparency document related to this article can be found online at <http://dx.doi.org/10.1016/j.cbi.2018.06.007>.

## References

- J.R. Nansseu, S.S. Ngo-Um, E.V. Balti, Incidence, prevalence and genetic determinants of neonatal diabetes mellitus: a systematic review and meta-analysis protocol, *Syst. Rev.* 5 (2016) 188.
- P.A. Diaz-Valencia, P. Bougneres, A.J. Valleron, Global epidemiology of type 1 diabetes in young adults and adults: a systematic review, *BMC Publ. Health* 15 (2015) 255–270.
- A. Chawla, R. Chawla, S. Jaggi, Microvascular and macrovascular complications in diabetes mellitus: distinct or continuum? *Indian J Endocrinol Metab* 20 (2016) 546–551.
- R. Torkington-Stokes, D. Metcalf, P. Bowler, Management of diabetic foot ulcers: evaluation of case studies, *Br. J. Nurs.* 25 (2016) S27–S33.
- Y.J. Rhou, F.R. Henshaw, M.J. McGill, S.M. Twigg, Congestive heart failure presence predicts delayed healing of foot ulcers in diabetes: an audit from a multi-disciplinary high-risk foot clinic, *J. Diabet. Complicat.* 29 (2015) 556–562.
- U.A. Okonkwo, L.A. DiPietro, Diabetes and wound angiogenesis, *Int. J. Mol. Sci.* 18 (2017).
- S. Babaei, M. Bayat, M. Nouruzian, M. Bayat, Pentoxifylline improves cutaneous wound healing in streptozotocin-induced diabetic rats, *Eur. J. Pharmacol.* 700 (2013) 165–172.
- P.R. Cavanagh, B.A. Lipsky, A.W. Bradbury, G. Botek, Treatment for diabetic foot ulcers, *Lancet* 366 (2005) 1725–1735.
- Z. Guo, The modification of natural products for medical use, *Acta Pharm. Sin. B* 7 (2017) 119–136.
- M. Yusuf, M. Shabbir, F. Mohammad, Natural colorants: historical, processing and sustainable prospects, *Nat Prod Bioprospect* 7 (2017) 123–145.
- Y. Kumagai, Y. Shinkai, T. Miura, A.K. Cho, The chemical biology of naphthoquinones and its environmental implications, *Annu. Rev. Pharmacol. Toxicol.* 52 (2012) 221–247.
- J. Bascha, B.R.S. Murthy, P.R. Likhitha, Y. Ganesh, B.G. Bai, R.J. Rani, P. Prakash, V. Shanmugham, A. Kirthi, In vitro and in vivo assessment of lawsone microsphere loaded chitosan scaffolds, *Int. J. Phytopharm.* 6 (2016) 74–84.
- M. Dong, D. Liu, Y.H. Li, X.Q. Chen, K. Luo, Y.M. Zhang, R.T. Li, Naphthoquinones from *Onosma paniculatum* with potential anti-inflammatory activity, *Planta Med.* 83 (2017) 631–635.
- E. Moreno, J. Schwartz, E. Larrea, I. Conde, M. Font, C. Sanmartin, J.M. Irache, S. Espuelas, Assessment of  $\beta$ -lapachone loaded in lecithin-chitosan nanoparticles for topical treatment of cutaneous leishmaniasis in *L. major* infected BALB/c mice, *Nanomed. Nanotechnol. Biol. Med.* 11 (2015) 9.
- F. Ourique, M.R. Kwiecinski, G. Zirbel, L. Castro, A.J. Gomes Castro, F.R. Mena Barreto Silva, J.A. Valderrama, D. Rios, J. Benites, P.B. Calderon, R.C. Pedrosa, In vivo inhibition of tumor progression by 5 hydroxy-1,4-naphthoquinone (juglone) and 2-(4-hydroxyanilino)-1,4-naphthoquinone (Q7) in combination with ascorbate, *Biochem. Biophys. Res. Commun.* 477 (2016) 640–646.
- A. Skrzypczak, N. Przystupa, A. Zgadzaj, A. Parzonko, K. Sykowska-Baranek, K. Paradowska, G. Nalecz-Jawewski, Antigenotoxic, anti-photogenotoxic and antioxidant activities of natural naphthoquinone shikonin and acetylshikonin and Arnebia euchroma callus extracts evaluated by the umu-test and EPR method, *Toxicol. Vitro* 30 (2015) 364–372.
- A. Richwien, G. Wurm, Inhibition of the arachidonic acid cascade by aza-2-aryl-1,4-naphthoquinone derivatives, *Pharmazie* 59 (2004) 906–912.
- P.K. Lakshmi, N. Thangellapalli, A. Chennuri, D. Prasanthi, D. Veeresh, Wound healing activity of topical lawsone gel on rat model, *Int. J. Pharmaceut. Sci. Res.* 59 (2017) 3162–3169.
- D.E. Pisani, M.J. Pointon, R.S. Pardini, Comparison of the effects on mitochondrial function of a series of 2-methyl substituted 1,4-naphthoquinones to their 6-methyl counterparts, *Biochem. Pharmacol.* 35 (1986) 2587–2591.
- V. Shneyvays, D. Leshem, Y. Shmist, T. Zinman, A. Shainberg, Effects of menadione and its derivative on cultured cardiomyocytes with mitochondrial disorders, *J. Mol. Cell. Cardiol.* 39 (2005) 149–158.
- T.P. Barbosa, H. Diniz Neto, Preparação de derivados do lapachol em meio ácido e em meio básico: uma proposta de experimentos para a disciplina de Química Orgânica Experimental, *Quim. Nova* 36 (2013) 331–334.
- T. Mosmann, Rapid colorimetric assay for cellular growth and survival: application to proliferation and cytotoxicity assays, *J. Immunol. Meth.* 65 (1983) 55–63.
- B.S. Herrera, A. Kantarci, A. Zarough, H. Hasturk, K.P. Leung, T.E. Van Dyke, LXa4 actions direct fibroblast function and wound closure, *Biochem. Biophys. Res. Commun.* 464 (2015) 1072–1077.
- J.L. Amorim, J.B. Figueiredo, A.C.F. Amaral, E.G.O. Barros, C. Palmero, M.P. MA, A.S. Ramos, J.L.P. Ferreira, J.R.A. Silva, C.F. Benjamim, S.L. Basso, L.E. Nasciutti, P.D. Fernandes, Wound healing properties of *Copaifera paupera* in diabetic mice, *PLoS One* 12 (2017) e0187380.
- M.D. Baldissera, C.F. Souza, T.H. Grando, L.F. Cossetin, M.R. Sagrillo, K. Nascimento, A.S. da Silva, A.K. Machado, I.B.M. da Cruz, L.M. Stefani, B. Klein, R. Wagner, S.G. Monteiro, Antihyperglycemic, antioxidant activities of tucuma oil (*Astrocaryum vulgare*) in alloxan-induced diabetic mice, and identification of fatty acid profile by gas chromatograph: new natural source to treat hyperglycemia, *Chem. Biol. Interact.* 270 (2017) 51–58.
- V. Nithaya, A.A. Baskar, A preclinical study on wound healing activity of lawsone alba linn, *Res. J. Phytochem.* 5 (2011) 123–129.
- V.P. Papageorgiou, A.N. Assimopoulou, A.C. Ballis, Alkannins and shikonins: a new class of wound healing agents, *Curr. Med. Chem.* 15 (2008) 3248–3267.
- F.I. Carroll, H. Wayne, M.R. Miller, Thiosemicarbazone and amidinohydrazone derivatives of some 1,4-naphthoquinones, *J. Chem. Soc. C Org.* 0 (1970) 1993–1996.
- V.R. Campos, E.A. Santos, V.F. Ferreira, R.C. Montenegro, M.C.B.V. Souza, V.C. Costa-Lotufo, M.O. Moraes, A.K.P. Refuge, A.K. Jordão, A.C. Pinto, J.A.L.C. Resende, A.C. Cunha, Synthesis of carbohydrate-based naphthoquinones and substituted phenylhydrazone derivatives as anticancer agents, *RSCAdvances* 2 (2012) 11438–11448.
- P. Costa, R. Pilli, S. Pinheiro, M. Vasconcelos, Substâncias carboniladas e derivados, (2003) 12–2003 ed.
- G.A.M. Jardim, W.J. Reis, M.F. Ribeiro, F.M. Ottoni, R.J. Alves, T.L. Silva, M.O.F. Goulart, A.L. Braga, R.F.S. Menna-Barreto, K. Salomão, S.L. Castro, E.N. Silva Júnior, On the investigation of hybrid quinones: synthesis, electrochemical studies and evaluation of trypanocidal activity, *RSC Adv.* 5 (2015) 78047–78060.
- R. Munday, B.L. Smith, C.M. Munday, Structure-activity relationships in the haemolytic activity and nephrotoxicity of derivatives of 1,2- and 1,4-naphthoquinone, *J. Appl. Toxicol.* 27 (2007) 262–269.
- L.N. Irazazabal, W.F. Porto, S.M. Ribeiro, S. Casale, V. Humblot, A. Ladram, O.L. Franco, Selective amino acid substitution reduces cytotoxicity of the antimicrobial peptide mastoparan, *Biochim. Biophys. Acta* 1858 (2016) 2699–2708.
- D.S. Glazer, R.J. Radmer, R.B. Altman, Improving structure-based function prediction using molecular dynamics, *Structure* 17 (2009) 919–929.
- P. Srinivas, C.R. Patra, S. Bhattacharya, D. Mukhopadhyay, Cytotoxicity of naphthoquinones and their capacity to generate reactive oxygen species is quenched when conjugated with gold nanoparticles, *Int. J. Nanomed.* 6 (2011) 2113–2122.
- G. Serini, M.L. Bochaton-Piallat, P. Ropraz, A. Geinoz, L. Borsi, L. Zardi, G. Gabbiani, The fibronectin domain ED-A is crucial for myofibroblastic phenotype induction by transforming growth factor- $\beta$ 1, *J. Cell Biol.* 142 (1998) 873–881.
- X.J. Liu, F.Z. Kong, Y.H. Wang, J.H. Zheng, W.D. Wan, C.L. Deng, G.Y. Mao, J. Li, X.M. Yang, Y.L. Zhang, X.L. Zhang, S.L. Yang, Z.G. Zhang, Lumican accelerates wound healing by enhancing  $\alpha$ 2 $\beta$ 1 integrin-mediated fibroblast contractility, *PLoS One* 8 (2013) e67124.
- C.C. Liang, A.Y. Park, J.L. Guan, In vitro scratch assay: a convenient and inexpensive method for analysis of cell migration in vitro, *Nat. Protoc.* 2 (2007) 329–333.
- M. Hirane, M. Araki, Y. Dong, K. Honoki, N. Fukushima, T. Tsujiuchi, Inhibitory effects of LPA1 on cell motile activities stimulated by hydrogen peroxide and 2,3-dimethoxy-1,4-naphthoquinone in fibroblast 3T3 cells, *Biochem. Biophys. Res. Commun.* 441 (2013) 47–52.
- H.N. Kung, M.J. Yang, C.F. Chang, Y.P. Chau, K.S. Lu, In vitro and in vivo wound healing-promoting activities of beta-lapachone, *Am. J. Physiol. Cell Physiol.* 295 (2008) C931–C943.
- P. Bannon, S. Wood, T. Restivo, L. Campbell, M.J. Hardman, K.A. Mace, Diabetes induces stable intrinsic changes to myeloid cells that contribute to chronic inflammation during wound healing in mice, *Dis Models Mech* 6 (2013) 1434–1447.
- R.E. Mirza, M.M. Fang, E.M. Weinheimer-Haus, W.J. Ennis, T.J. Koh, Sustained inflammasome activity in macrophages impairs wound healing in type 2 diabetic humans and mice, *Diabetes* 63 (2014) 1103–1114.
- M.R. Dasu, S. Devaraj, I. Jialal, High glucose induces IL-1 $\beta$  expression in human monocytes: mechanistic insights, *Am. J. Physiol. Endocrinol. Metab.* 293 (2007) E337–E346.
- R.E. Mirza, M.M. Fang, W.J. Ennis, T.J. Koh, Blocking interleukin-1 $\beta$  induces a healing-associated wound macrophage phenotype and improves healing in type 2 diabetes, *Diabetes* 62 (2013) 2579–2587.
- M.F. Siqueira, J. Li, L. Chehab, T. Desta, T. Chino, N. Krothpali, Y. Behl, M. Alikhani, J. Yang, C. Braasch, D.T. Graves, Impaired wound healing in mouse models of diabetes is mediated by TNF- $\alpha$  dysregulation and associated with enhanced activation of forkhead box O1 (FOXO1), *Diabetologia* 53 (2010) 378–388.
- S.A. Chen, H.M. Chen, Y.D. Yao, C.F. Hung, C.S. Tu, Y.J. Liang, Topical treatment with anti-oxidants and Au nanoparticles promote healing of diabetic wound through receptor for advance glycation end-products, *Eur. J. Pharmaceut. Sci.* 47 (2012) 875–883.
- G.S. Sidhu, A.K. Singh, K.K. Banauha, J.P. Gaddipati, G.K. Patnaik, R.K. Maheshwari, Arnebin-1 accelerates normal and hydrocortisone-induced impaired wound healing, *J. Invest. Dermatol.* 113 (1999) 773–781.
- Z. Zeng, B.H. Zhu, Arnebin-1 promotes the angiogenesis of human umbilical vein endothelial cells and accelerates the wound healing process in diabetic rats, *J. Ethnopharmacol.* 154 (2014) 653–662.